Supplemental Material

Supplemental Figure S1

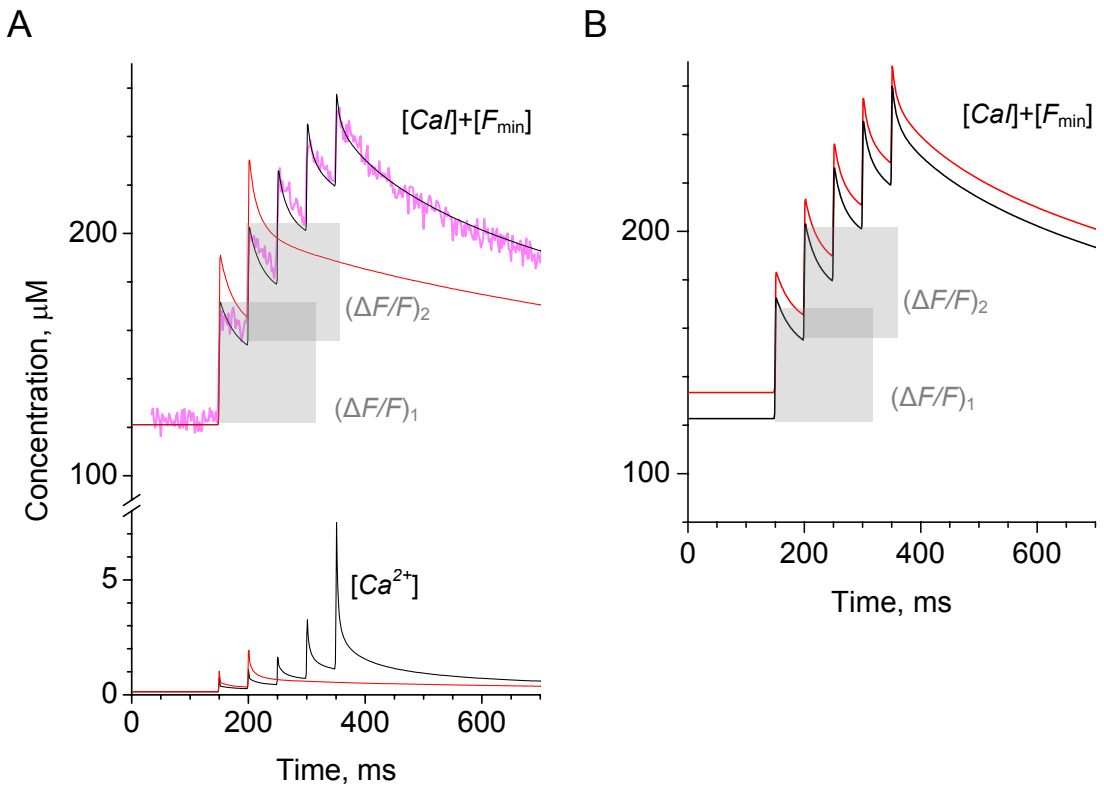

Figure S1. In giant MF boutons, moderate fluctuations in the action potential induced Ca^{2+} entry or in the baseline Ca^{2+} level have a relatively small effect on the paired-pulse ratio (PPR) of the first two Ca^{2+} -dependent fluorescence responses, PPR = $(\Delta F/F)_2 / (\Delta F/F)_1$.

A, Notations [*Cal*]+[F_{min}] and [Ca^{2+}] stand for the effective concentration of, respectively, the Ca^{2+}-bound indicator Fluo-4 (which reflects the recorded fluorescence signal including baseline fluorescence) and the calculated free intra-terminal Ca^{2+}. Magenta trace, the average recorded presynaptic Ca^{2+} signal at MF - CA3 pyramidal cell synapses in control conditions, as determined previously (Scott and Rusakov, 2006). Black lines, model prediction in baseline conditions. Red lines, model prediction in test conditions, namely a 35% increase in the action potential dependent Ca^{2+} entry. The difference in PPR between baseline and test condition is

only ~10% (*ΔF/F* values measured in baseline conditions are depicted by gray rectangles).

Calculations were carried out using a one-compartment kinetic model of multi-component, non-stationary reactions of Ca^{2+} entry, binding and extrusion, as detailed earlier (Scott and Rusakov, 2006). The main parameters were: Ca^{2+} indicator, 200 μM Fluo-4; endogenous buffer, 160 μM calbindin-28k (K_d = 300 nM); resting Ca^{2+} concentration, 110 nM; total spike evoked cytosolic Ca^{2+} entry in baseline conditions, 50 μM; Ca^{2+} removal rate, P = 0.37.

B, Black lines, baseline conditions, as in *A*; red lines, test condition: a 20% increase in the resting Ca^{2+} concentration. The resulting difference in the PPR values between baseline and test condition is ~1%. Other notations are as in *A*.

Supplemental Figure S2

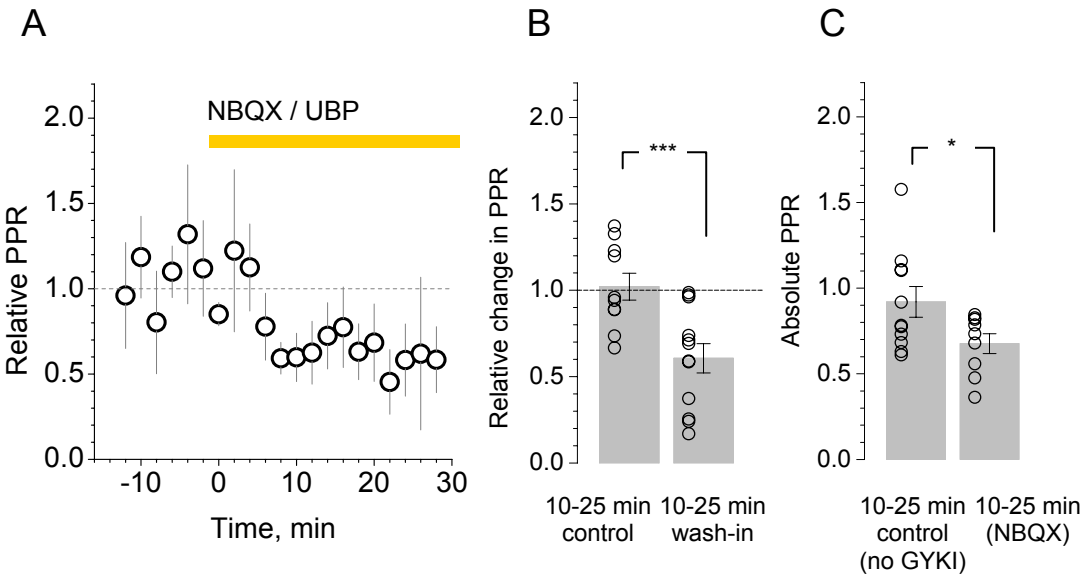

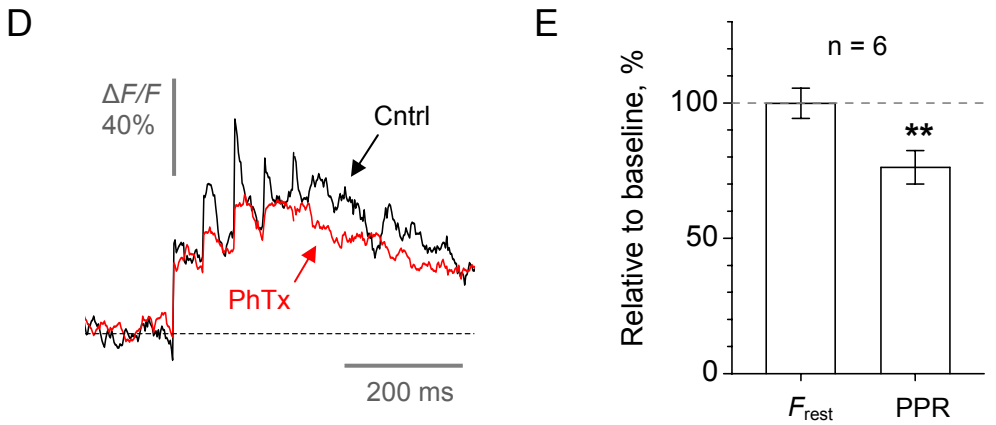

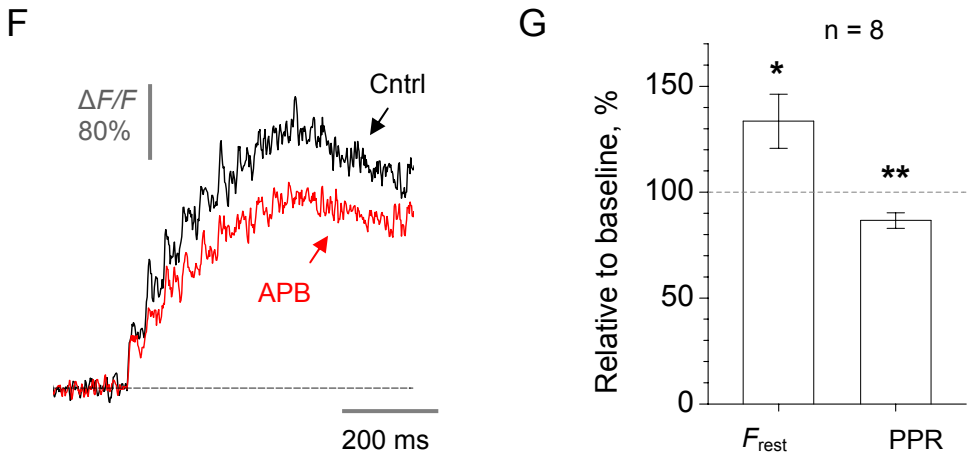

Figure S2. Pharmacological blockade of KARs and Ca^{2+} stores decreases the paired-pulse ratio of action-potential-induced Ca^{2+} responses, PPR = $(\Delta F/F)_2$ / $(\Delta F/F)_1$, in giant MF boutons in area CA3.

A, The average time course of the KAR blockade effect on the PPR in giant MF boutons (n = 12, NBQX and UBP302 data combined; also see Fig. 1*E*) showing a robust reduction in the PPR;

B-C, Statistical summary of the KAR-dependent change in the PPR among experimental groups with matched timing of measurements. *B*, A control group of giant CA3 MF boutons (in the presence of GYKI) shows no detectable changes in PPR over a 10-25 min interval of recording (average change: 2 ± 8%, n = 10). In contrast, blockade of KARs reduces PPR by 39 ± 8 % (n = 12, $p < 0.005$) within a similar time interval following wash-in of the drug (NBQX or UBP302). *C*, The absolute PPR values in a control group (of giant MF boutons in area CA3) are larger than in the group exposed to NBQX (average PPRs, respectively: 0.92 ± 0.09 and 0.68 ± 0.06, n = 8 and n = 11, difference at $p < 0.04$).

D, Blocking Ca^{2+} permeable KARs wih philanthotoxin (PhTx) reduces the PPR of action potential evoked presynaptic Ca^{2+} transients in giant MF boutons in CA3. Characteristic recordings from a single giant MF bouton, before (black) and 15 min after application of philanthotoxin (3 μM), in response to five action potentials at 20 Hz evoked at the soma (traces: 10-trial average; see Materials and Methods for Ca^{2+} imaging methods).

E, Statistical summary of experiments shown in *D*: Average values (± SEM) of the resting Ca^{2+} -dependent fluorescence (F_{rest}; change 0.2 ± 5.6%, n = 6, $p > 0.95$) and paired-pulse ratio (PPR, change −24 ± 6%, $p < 0.01$) of the two first spike-evoked presynaptic Ca^{2+} responses (as in Fig. 1 of the main text) after PhTx application, relative to the values prior to the application. **, $p < 0.01$.

F, The Ca^{2+} store IP_3 receptor blocker 2-Aminoethoxydiphenyl borate (2-APB) reduces the PPR of action-potential-evoked presynaptic Ca^{2+} responses in giant MF boutons in area CA3. Characteristic recordings of Ca^{2+}-dependent fluorescence (Fluo-4) in control conditions (black) and following application of 2-APB (red; 10 action potentials at 20 Hz; see Fig. 1 and Materials and Methods for Ca^{2+} imaging methods).

G, Summary of average effects in experiments shown in *F* (*, $p < 0.05$; **, $p < 0.01$). Note that the overall difference between presynaptic Ca^{2+} signals with and without IP_3-dependent stores blocked (the difference between the two curves) is consistent with the large Ca^{2+} store signal evoked by incaging IP_3 in individual boutons (Fig. 5 of the main text).

Supplemental Figure S3

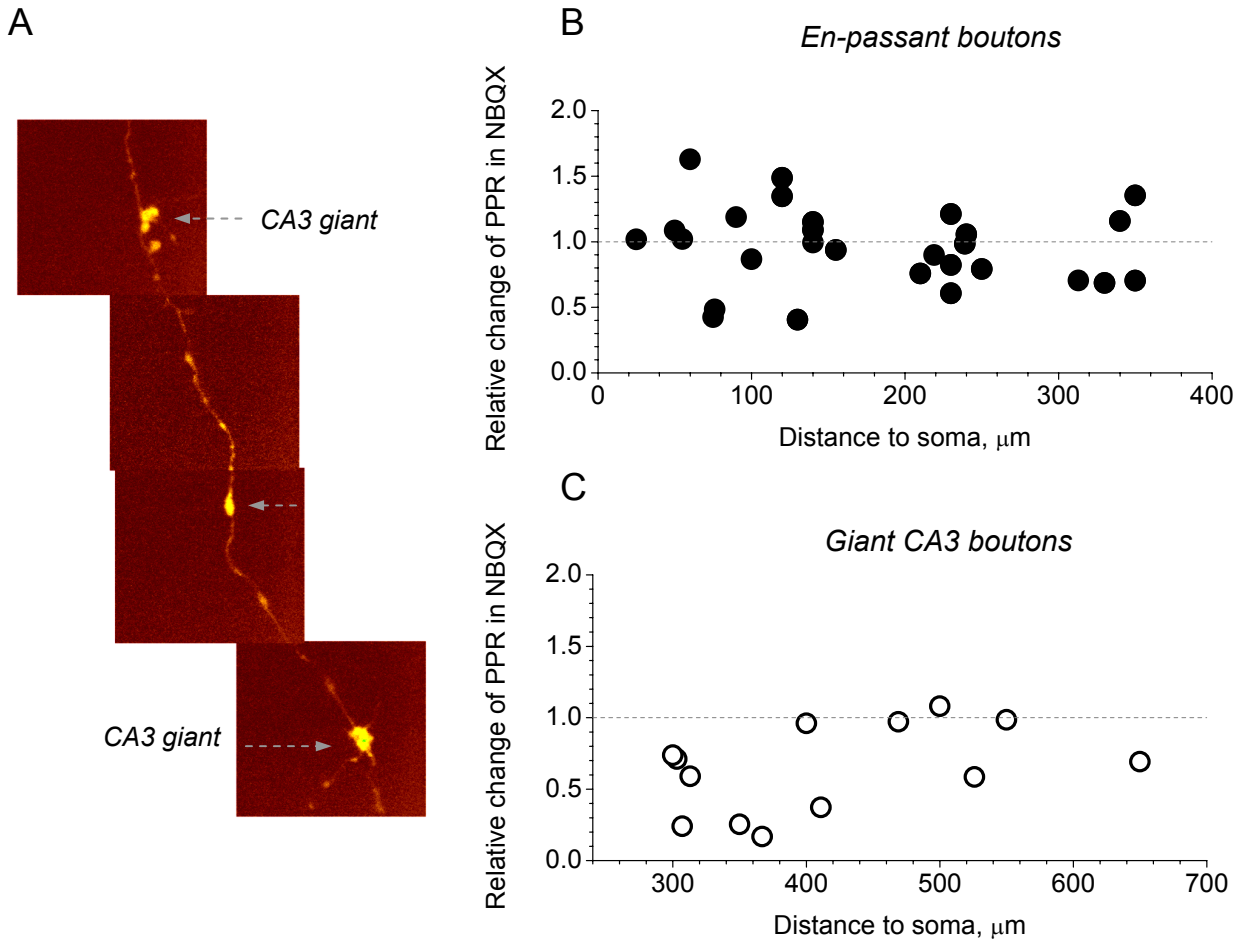

Figure S3. The effect of KAR blockade on the paired-pulse ratio of presynaptic Ca^{2+} signals, PPR = $(\Delta F/F)_2 / (\Delta F/F)_1$ (two action potentials 50 ms apart), does not depend on the bouton-soma distance.

A, A reconstructed fragment of an axon illustrating en-passant boutons that occur between giant MF boutons in area CA3.

B, Relative change in the PPR recorded in en-passant boutons following blockade of KARs by NBQX. The data show no linear regression for the effect versus distance ($p > 0.5$; average change: −6 ± 6%, n = 29).

C, Relative change in the PPR recorded in giant CA3 boutons following blockade of KARs. The visible *decrease* of the effect with distance to the soma is insignificant (regression at $p > 0.13$; average change: −36 ± 9%, n = 13).

Supplemental Figure S4

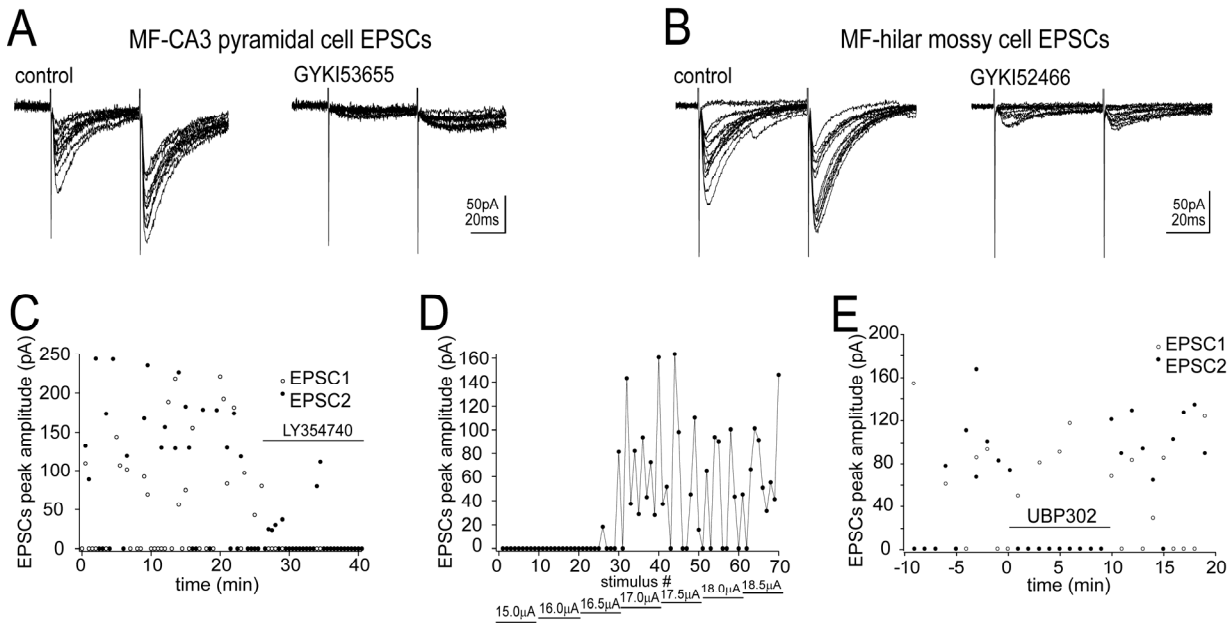

Figure S4. Documenting the KAR sensitivity of EPSCs in MF target cells.

A, Contribution of non-AMPA (and non-NMDA) receptor-mediated currents to EPSCs in hilar mossy cells. One cell examples are shown. Application of the AMPA selective antagonist GYKI53655 (50 μM) strongly reduced EPSCs recorded in a mossy cell (left panel; NMDA receptors were blocked with 50 μM APV from the start), unmasking a much smaller, slower synaptic current component (right panel).

B, An experiment similar to that shown in *A* but carried out in CA3 pyramidal cells; the effect of the AMPA selective antagonist GYKI52466 (50 μM) is shown.

C, Amplitudes of EPSCs evoked by single MF stimulation (minimal stimulation protocol) in a CA3 pyramidal cell. Paired-pulse responses (20 Hz) are shown as EPSC1 and EPSC2; see main text Fig. 6 for characteristic examples. EPSC1 and EPSC2 display stable amplitudes and failure rates over the 25 min recording session. Subsequent application of the group II mGluR agonist LY354740 (0.5 μM, indicated) abolished the responses.

D, The amplitude of EPSCs evoked by minimal stimuli in a CA3 pyramidal cell was not affected by moderate variation in the stimulation intensity.

E, Time course of the effect of UBP302 on minimal stimulation responses, as indicated. A clear and reversible reduction in the occurrence of EPSC2 successes is seen. One cell examples are shown in *C-E*.

Supplemental Table S1.

Parameter	CA3 pyramidal cells	Hilar mossy cells	Hilar interneurons
EPSC1 failure rate, %	68.3 ± 6.7 65.1 ± 10.3	35.4 ± 5.0 37.5 ± 7.9	39.0 ± 10.4 36.5 ± 8.5
EPSC2 failure rate, %	37.7 ± 7.6 **51.3 ± 11.5****	13.7 ± 2.5 20.1 ± 6.3	26.5 ± 11.2 26.3 ± 13.9
Paired-pulse ratio including failures	3.1 ± 0.6 **2.1 ± 0.3***	2.3 ± 0.2 2.3 ± 0.2	1.7 ± 0.2 1.8 ± 0.2
EPSC1 peak amplitude with failures, pA	31.3 ± 5.4 26.1 ± 8.0	53.0 ± 9.5 46.3 ± 9.6	50.8 ± 24.0 42.3 ± 13.0
EPSC2 peak amplitude with failures, pA	87.4 ± 11.2 **59.9 ± 11.8****	110.7 ± 13.6 96.6 ± 19.4	74.7 ± 14.6 68.7 ± 27.1
EPSC1 peak amplitude without failures, pA	99.2 ± 18.1 60.6 ± 17.8	80.1 ± 8.9 68.9 ± 7.8	86.0 ± 7.3 67.0 ± 7.9
EPSC2 peak amplitude without failures, pA	155.7 ± 18.1 **121.3 ± 11.5***	125.7 ± 14.3 112.7 ± 17.1	102.0 ± 5.3 95.0 ± 5.7
Sample size	n = 11	n = 11	n = 11

Data summary for paired-pulse minimal stimulation experiments in three types of MF target cells, as indicated. In the table, upper (black) and lower (red) lines correspond to control conditions and those following application of 10 μM UBP302. Mean ± SEM are shown; *, $p < 0.05$; **, $p < 0.01$ (non-parametric Wilcoxon paired test). See main text Fig. 6 for further details.

REFERENCES

Cossart R, Epsztein J, Tyzio R, Becq H, Hirsch J, Ben-Ari Y, Crepel V (2002) Quantal release of glutamate generates pure kainate and mixed AMPA/kainate EPSCs in hippocampal neurons. Neuron 35:147-159.

Miller LD, Petrozzino JJ, Connor JA (1995) G protein-coupled receptors mediate a fast excitatory postsynaptic current in CA3 pyramidal neurons in hippocampal slices. J Neurosci 15:8320-8330.

Scott R, Rusakov DA (2006) Main determinants of presynaptic Ca^{2+} dynamics at individual mossy fiber-CA3 pyramidal cell synapses. J Neurosci 26:7071-7081.